

Crystallization of amorphous Te-20 at % Sn alloy

M. KACZOROWSKI*, J. KOZUBOWSKI, B. DABROWSKI, H. MATYJA
*Institute of Materials Science and Engineering, Warsaw Technical University, Narbutta 85,
 02-524 Warsaw, Poland*

Amorphous Te–20 at % Sn alloy was obtained by rapid cooling from the liquid state. Phase transitions occurring during continuous heating of amorphous films were studied by differential thermal analysis, X-ray diffraction and transmission electron microscopy. It was found that the crystallization of the amorphous phase begins at 382 K and proceeds via nucleation and growth of metastable phases MS1 and MS2. The first of these phases was assigned the primitive cubic structure with lattice parameter $a = 3.2 \text{ \AA}$. The second phase, being a Te (Sn) solution, was assigned the hexagonal structure with lattice parameters $a = 4.45 \text{ \AA}$ and $c = 5.85 \text{ \AA}$. During heating at 410 K the remaining amorphous phase decomposed into a mixture of Te crystals together with metastable phase MS3, which probably has the ZnS type structure with lattice parameter $a = 6.05 \text{ \AA}$. Within the temperature range 450 to 550 K the MS1 phase was transformed into SnTe, and the MS2 phase into Te. The metastable intermediate phase MS3 decomposed only near the solidus temperature, and the alloy attained its equilibrium structure.

1. Introduction

Tellurium forms homologous phase equilibrium systems with group IV elements characterized by so-called deep-well type eutectics. A study was made of $\text{Te}_{100-x}\text{A}_x$ (IV) alloys where x is the alloying element content, with special consideration given to alloys which can most easily be obtained in the amorphous state by rapid cooling from the liquid state. In earlier studies we have described crystallization of amorphous tellurium $\text{Te}_{100-x}\text{Pb}_x$ ($x = 15$ to 30) [1] and Te–20 at % Pb [2] alloys. In this paper results of crystallization studies of the amorphous alloy Te–20 at % Sn are presented.

2. Experimental

The alloy was prepared by melting of the appropriate amounts of components (total weight 10 g) in a quartz ampoule under a vacuum of 10^{-5} torr. The purity of the components was 5N. Melting was repeated several times at a temperature exceeding the liquidus temperature by 100 K. The

duration of each melting was 0.5 h. Rapid cooling was achieved by the gun method, with the use of apparatus resembling that described by Duwez and Willens [3]. The alloy (~ 5 mg) was melted at 873 K and then ejected by an argon shock wave ($p = 22$ atm) onto a backing made of material with high surface film conductance. Copper and silver backings were used.

Immediately after rapid cooling the alloy structure was investigated by diffractometry and electron microscopy. Diffractometric studies were performed on a Phillips PM 8000 diffractometer, with the use of $\text{CoK}\alpha$ radiation; microscopic observations were made in a Philips EM 300 transmission electron microscope.

Calorimetric measurements were taken in a Perkin Elmer DSC-2 differential microcalorimeter at a heating rate $V_g = 20 \text{ K min}^{-1}$. After determination of the temperatures of the different transitions, the thermal treatment of the specimens destined for diffractometric and microscopic

*Present address: Institute of Casting, Welding and Bulk Metal Forming, Warsaw Technical University, Narbutta 85, 02-524 Warsaw, Poland.

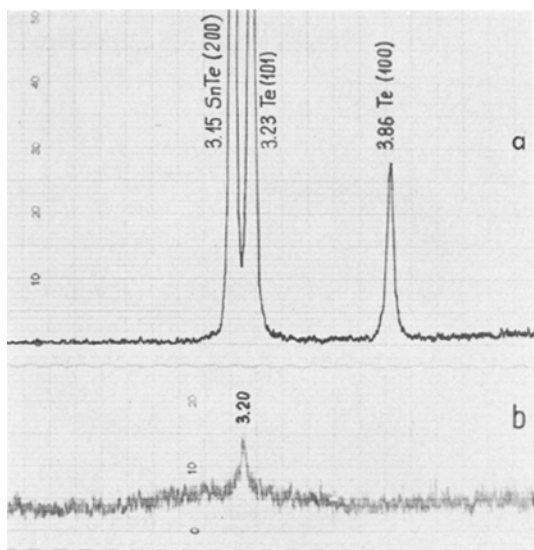


Figure 1 Fragments of X-ray diffraction patterns for (a) equilibrium and (b) as-quenched Te–20 at % Sn alloy.

tests was programmed. Foils assigned for these studies were heated under argon, at a heating rate of 20 K min^{-1} .

Structures of the metastable intermediate phases were identified on the basis of the results of X-ray diffraction and electron diffraction studies. In the case of electron diffraction the method of reciprocal lattice reconstruction was applied; for this purpose use was made of a series of diffraction patterns, recorded for the same crystal rotated around one of the main crystallographic directions.

3. Results

A part of an X-ray diffractogram obtained for the alloy immediately after rapid cooling is presented in Fig. 1. A diffuse maximum characteristic of non-crystalline materials is visible in the figure. In addition to this maximum, a fairly distinct reflection originating from the crystalline phase, indicating that the alloy has not been obtained in the amorphous state in its whole volume, is present in the diffractogram. This reflection corresponds to an interplanar distance $d = 3.20 \text{ \AA}$, which occurs in neither of the two equilibrium phases ($d_{200}^{\text{SnTe}} = 3.15 \text{ \AA}$, $d_{101}^{\text{Te}} = 3.23 \text{ \AA}$) and probably originates from a metastable phase. Due to the small number of reflections (only two altogether), the XRD method permits no identification of the structure of this phase.

Figs. 2a and b present the electron micrographs of the alloy structure after rapid cooling, observed in bright and dark fields respectively. The dark-field picture is obtained from a part of the ring marked with a circle in the diffraction pattern (Fig. 2a), using the method of beam inclination.

According to Fig. 2a, after rapid cooling the alloy shows no crystalline structure in the thin areas; this is confirmed by the electron diffraction pattern with diffuse rings analogous to the diffuse maximum in the X-ray diffractogram (Fig. 1). In the dark-field micrographs (Fig. 2b) bright spots of mean size of 15 to 20 Å are visible, providing proof that coherently scattered regions are not larger than this; Rudee [4] and Howie *et al.* [5] suggest that such spots can be interpreted as proof of the microcrystalline structure of foils.

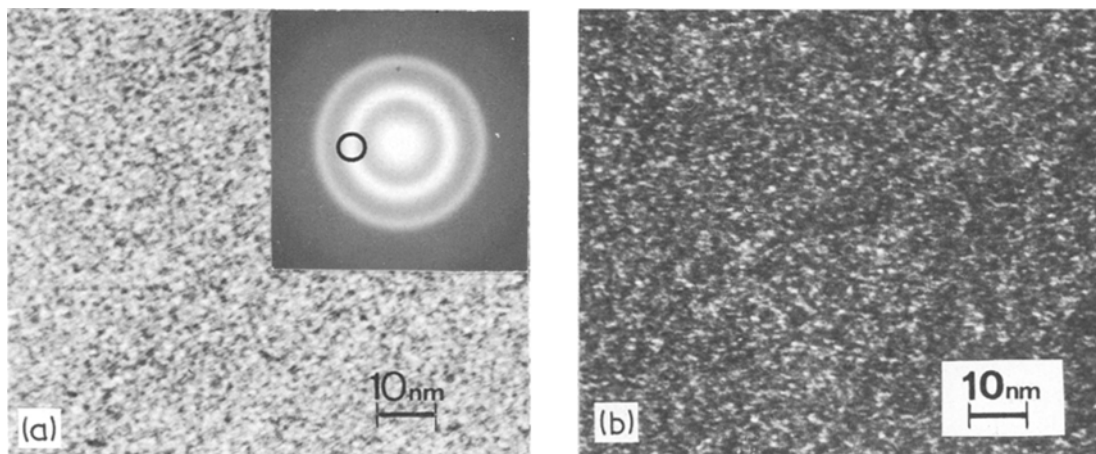


Figure 2 (a) TEM bright-field and diffraction pattern of as-quenched foil; (b) dark-field of the same area.

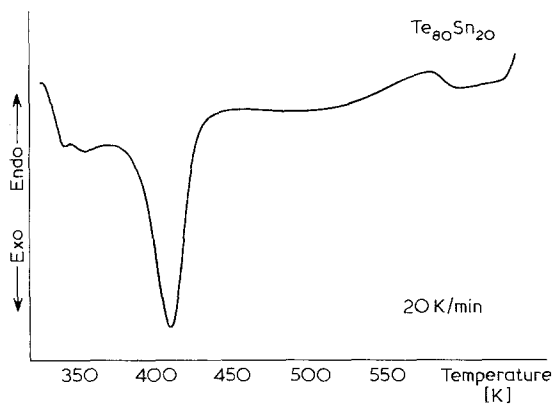


Figure 3 Typical DSC curve at a scanning rate of 20 K min^{-1} .

However, according to Herd *et al.* [6], the occurrence of these bright spots in dark-field micrographs is not sufficient evidence for a microcrystalline structure, since identical micrographs may be obtained for structures with dense random packing of atoms [7].

4. Annealing behaviour

4.1. Calorimetry

Fig. 3 shows a thermogram obtained for Te–20 at% Sn heated at a rate of 20 K min^{-1} . The thermogram records four thermal effects whose temperatures, determined by the intersection points of the corresponding tangents, are;

$$T_1 = 356 \text{ K}$$

$$T_2^{\text{P}} = 383 \text{ K} \quad \text{where } T_i^{\text{P}} = \text{temperature}$$

$$T_3^{\text{P}} = 463 \text{ K} \quad \text{of beginning of } i\text{th transi-}$$

$$T_4^{\text{P}} = 580 \text{ K} \quad \text{tion}$$

As to the course of the initial segment of the DSC curve, it is concluded that the first thermal effect most likely corresponds to the glass transition temperature T_g . This conclusion arises from the fact that the results of X-ray diffractometric and electron microscopic studies of alloys heated to the temperature $T_1 + 10 \text{ K}$, and maintained at this temperature for 30 sec do not differ perceptibly from the results obtained for this alloy immediately after rapid cooling. The second thermal effect corresponds to the crystallization of amorphous Te–20 at% Sn alloy. Unfortunately, the alloy is not amorphous in its whole volume and thus the heat of crystallization cannot be determined. The third and fourth thermal effects,

preceding the attainment of the equilibrium structure by the alloy, will be discussed below.

4.2. X-ray diffraction

Diffractometric studies were performed on powdered specimens heated at 20 K min^{-1} . Fig. 4a shows an X-ray diffractogram of the alloy heated to 439 K. On account of the considerable diffuseness of the diffraction maxima, this diffractogram is very difficult to interpret. However, close analysis of the occurrence of the different reflections shows that their distribution is characteristic of the hexagonal structure of tellurium. The shift of some reflections indicates that the phase formed during the crystallization of amorphous Te–20 at% Sn alloy is a Te (Sn) solution rather than pure Te. The calculated lattice parameters of this phase (referred to as MS2) are: $a = 4.45 \text{ \AA}$ and $c = 5.85 \text{ \AA}$. The calculated interplanar distances and those read from the diffractogram are recorded in Table I.

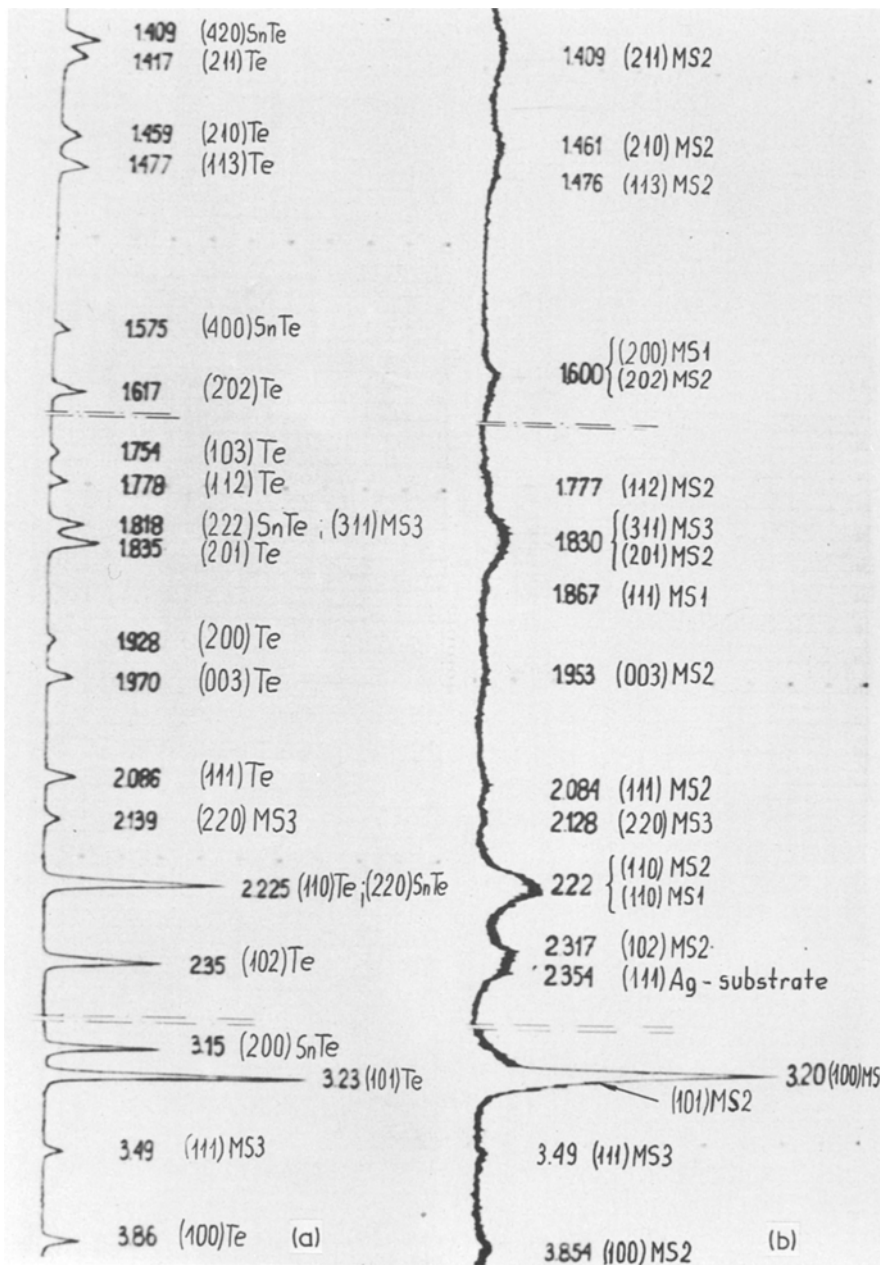
The existence of phase MS2 does not, however, account for the origin of the reflections corresponding to interplanar distances $d = 3.20 \text{ \AA}$ and $d = 1.600 \text{ \AA}$. These reflections are most probably due to another metastable phase which – to make a distinction – is referred to as MS1. The reflection corresponding to the interplanar distance $d = 3.20 \text{ \AA}$ undergoes no shift relative to the reflection from the crystalline phase observed side by side with the diffuse maximum in the diffractogram shown in Fig. 1. This suggests that the structure of phase MS1 formed during crystallization of amorphous Te–20 at% Sn alloy is either similar to or identical to that of the crystalline phase formed along with the amorphous phase upon rapid cooling from the liquid state.

TABLE I

No.	Miller indices	Interplanar distance	
		calculated	measured
1	100	3.85	3.85
2	101	3.22	3.22*
3	102	2.33	2.32
4	110	2.22	2.22
5	111	2.08	2.08
6	003	1.95	1.95
7	200	1.927	–
8	201	1.830	1.830
9	112	1.775	1.777
10	103	1.740	–

*Reflection masked by a very strong maximum corresponding to $d_{hkl} = 3.20 \text{ \AA}$.

Figure 4 X-ray diffraction patterns of alloy heated (a) to 510 K and (b) to 439 K.



The diffractogram shown in Fig. 4b was obtained for the alloy heated to 510 K. It exhibits distinct reflections from Te and SnTe; moreover, there are two additional "foreign" reflections corresponding to interplanar distances $d = 3.49 \text{ \AA}$ and $d = 2.14 \text{ \AA}$. These reflections, though still very faint, are evident already in the first diffractogram (Fig. 4a), indicating that the formation of the phase from which they are derived (referred to as MS3) begins before the end of the first

crystallization stage (400 K). Phase MS3 disappears only after heating of the alloy to 660 K, at which temperature the alloy attains its equilibrium structure.

4.3. Electron microscopy

Fig. 5 shows the structure of the alloy heated to 382 K. In the electron micrograph grains randomly distributed in the amorphous matrix are visible. Sometimes they form agglomerates comprising

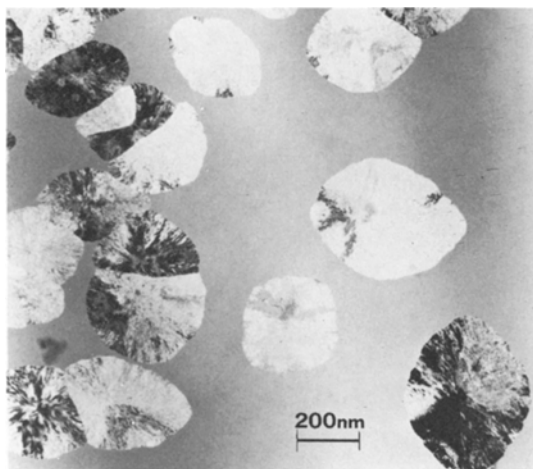


Figure 5 TEM micrograph of alloy heated to 382 K.

two or more grains. This may be due to the fact that the boundary of the earlier formed grains is a site preferred for nucleation and growth of the subsequent grains. The often observed characteristic differentiation in contrast within these agglomerates permits the assumption that the grains are twinned in the growth plane. Grains observed in the micrographs are characterized by the occurrence of strain contrasts caused by the presence of ultradispersed precipitates of another phase (Figs. 6a and b). The diffractogram (Fig. 6c) clearly testifies to the two-phase structure of the grains. A single "grain" is a mixture of phases; one of these phases has the primitive cubic structure of $Po\alpha$ type and lattice parameter $a = 3.2 \text{ \AA}$ (this phase gives rise to more intense reflections), whereas the other phase has a hexagonal structure with parameters $a = 4.45 \text{ \AA}$ and $c = 5.85 \text{ \AA}$. The crystallographic relationships between the phases can be expressed as:

$$\langle 111 \rangle_C \parallel \langle 101 \rangle_H \text{ and } \langle 211 \rangle_C \parallel \langle 100 \rangle_H$$

(C = cubic, H = hexagonal).

These relationships, often observed during the precipitation of a hexagonal phase within a cubic phase [8], seem to confirm the validity of the present structural analysis. Fig. 6b shows the dark-field picture obtained for the reflection $\langle 001 \rangle$ from the hexagonal phase. The picture reveals bright spots (mean size 30 to 50 \AA) indicating a dense pattern of precipitates on $\{111\}$ type planes of phase MS1.

The following photograph (Fig. 7) shows the structure of Te–20 at% Sn alloy heated to 410 K, i.e. to the temperature at which the transition rate attains a maximum (Fig. 3). Grains with two completely distinct morphologies are observed in the micrograph. In addition to the grains formed in the initial period of crystallization (Figs. 5 and 6), there are some later-formed crystals with a fairly regular shape, which are a mixture of Te crystals and phase MS3. During further heating of the alloy the precipitates in the two-phase areas, a mixture of MS1 and MS2, gradually increase (Fig. 8). According to the diffraction patterns, this process is paralleled by the transition of phase MS1 to SnTe compounds, and of phase MS2 to Te. However, phase MS3 still remains within the structure of the alloy; this is proved by the "additional" rings in the diffraction patterns obtained from the polycrystalline areas. This phase disappears only after heating the foil to 650 K. A structure typical of this stage of the transition is shown in Fig. 9. It is nearly free of dislocations, and twinning is observed in only some places.

5. Discussion

Results of the calorimetric and structural studies seem to indicate that under conditions of continuous heating the transition from the amorphous structure to the equilibrium crystalline structure proceeds through the following three stages:

(1) During the first stage, beginning at 383 K, the nucleation and growth of the crystalline phases take place. At first the grains are a mixture of metastable intermediate phases MS1 and MS2, and subsequently Te crystals and phase MS3 are formed.

(2) The second stage consists of diffusion processes during which SnTe compound is formed from phase MS1, and tellurium from phase MS2.

(3) The third stage, occurring near the solidus temperature, most likely comprises a polymorphic transition of metastable intermediate phase MS3 to equilibrium SnTe compound.

According to Turnbull's suggestions, crystallization by way of nucleation and growth can be indirect proof of the true amorphous structure of the starting material. The amorphous structure of the alloy immediately after rapid cooling is confirmed also by the fairly strong exothermic effect observed in the thermogram (Fig. 3). The

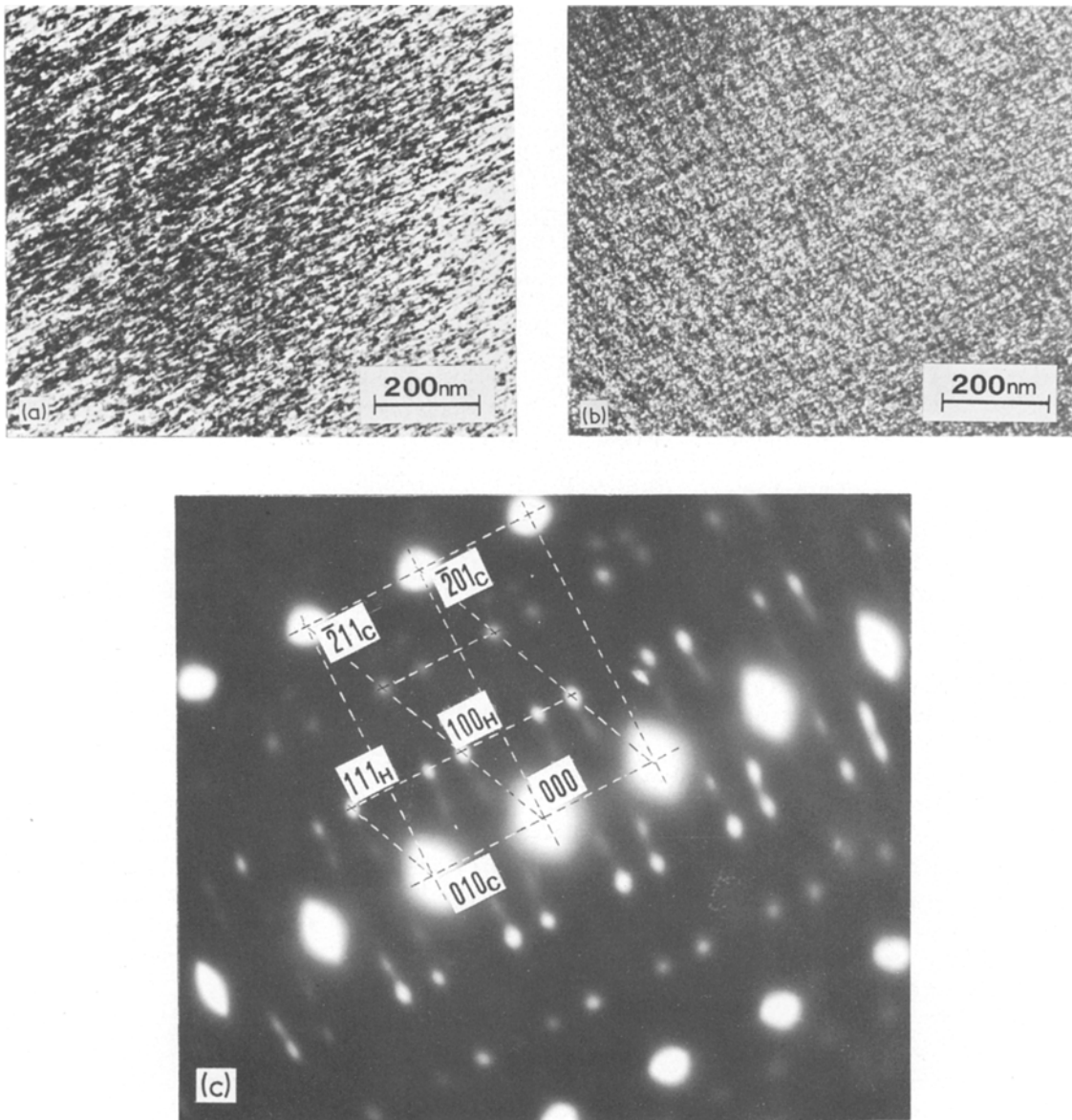


Figure 6 TEM (a) bright-field and (b) dark-field micrograph (high magnification) and (c) diffraction pattern of single crystal.

grains formed are paracrystals of phase MS1 in which areas with a “good” lattice, aligned in the $\langle 100 \rangle$ direction, have the shape of platelets or filaments which are several hundredths of Ångstroms long and 30 to 50 Å thick. Phase MS1, according to diffraction studies, has the primitive cubic structure with lattice parameter $a = 3.2 \text{ Å}$.

This phase, according to a suggestion by Giessen [9], can be considered to be the disordered compound SnTe supersaturated with tellurium atoms. In grains of phase MS1 on the $\{111\}$ planes, microcrystals of phase MS2 with hexagonal struc-

ture and lattice parameters $a = 4.45 \text{ Å}$ and $c = 5.85 \text{ Å}$ are present. Phase MS2 can be regarded as tellurium supersaturated with Sn atoms which occupy some nodes in the Te chains and cause contraction of the c parameter ($5.926 \rightarrow 5.85 \text{ Å}$). This contraction may be due to the attractive interactions between the tin and tellurium atoms, causing reduction of the angle between bonds. The shape of the microcrystals of phase MS2 is spheroidal and their size is ~ 30 to 50 Å (Fig. 6b). The high dispersion of phase MS2 explains the diffuseness of reflections in the diffractogram

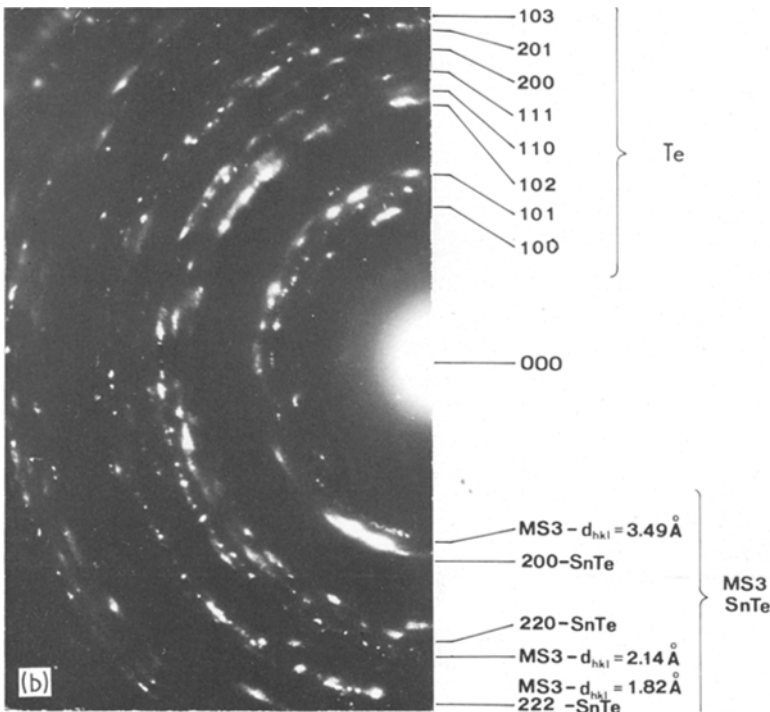


Figure 7 (a) TEM micrograph of alloy heated to 410 K, (b) corresponding diffraction pattern.

(Fig. 4a). Despite the existence of a definite crystallographic relationship between phases MS1 and MS2, which is typical of the processes of hexagonal phase precipitation within the matrix with cubic structure, in the present study precipitation of phase MS2 within the earlier crystallizing phase MS1 was in no case observed. The question

arises why the diffractogram in Fig. 4a shows the presence of only reflection $\{100\}$ from phase MS1, but not of other reflections, e.g. $\{100\}$ or $\{111\}$. This is probably due to the specific structure of the phase MS1 grains growing within the amorphous matrix. If the amorphous phase with mean ratio of Te:Se atoms of 4:1 is assumed to

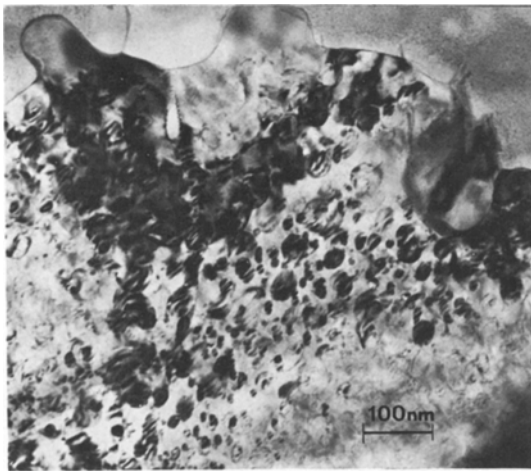


Figure 8 Growth of precipitates in two-phase region (MS1 + MS2) after heating of foils to 550 K.

exhibit microfluctuations in its composition, then these fluctuations could be expected to occur also in the metastable intermediate phase, MS1 crystallizing from the former. These microfluctuations would cause lattice deformations, and consequently a change in the interplanar distances. As a result, instead of closely defined distances between planes of the same type, the whole spectrum of distances d_{hkl} should be obtained. This fact would cause the diffuseness of reflections in the diffractogram; the degree of this diffuseness would be higher, the greater the order of the reflection and the larger the lattice deformation. Other factors partly explaining the absence of reflections $\{1\ 1\ 0\}$ and $\{1\ 1\ 1\}$ in the diffractogram

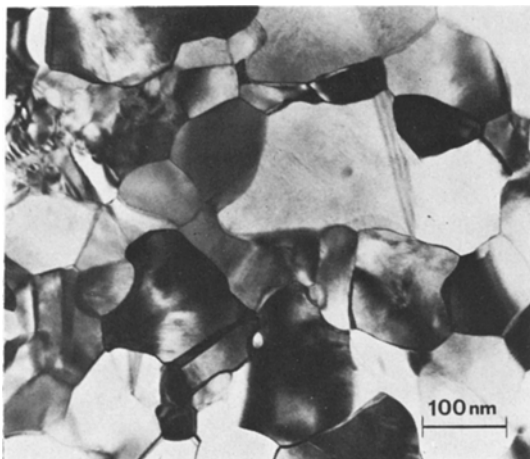


Figure 9 TEM micrograph of equilibrium structure of alloy.

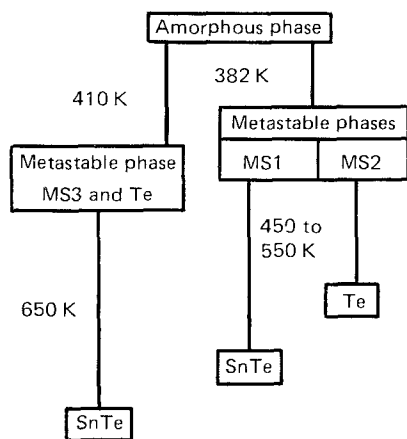
of Fig. 4a are the overlapping of the diffuse reflections from phase MS2 and of reflections $\{1\ 1\ 0\}$ and $\{1\ 1\ 1\}$ from phase MS1, as well as the unfavourable value of the Lorentz polarization factor, which for reflections with these indices is nearly half as much as for the reflection $\{1\ 0\ 0\}$.

During further heating of the alloy the phase MS2 precipitates increase. This increase proceeds via an addition of Te atoms leaving phase MS1 by diffusion, so that this phase becomes less rich in Te. In parallel, Sn atoms supersaturating the metastable phase MS2 leave it and pass to phase MS1. Both these processes, which are controlled by diffusion at the interphase boundary, result in the gradual transition of phase MS1 to SnTe compound and of phase MS2 to Te.

Formation of phase MS3, being a product of the decomposition (at 410 K) of the residual amorphous phase, is fairly unexpected. Probably this phase is formed because the crystallization process is carried out under conditions of continuous heating, and thus at various temperatures different mechanisms determine the nature of the glass-to-crystal transition. Comparison of the experimentally determined ratios of the interplanar distances with the ratios tabulated by Jouffrey [10] indicates that phase MS3 may have a cubic structure with lattice parameter $a = 6.05 \text{ \AA}$. The fact that from the time of its formation till the attainment of the equilibrium structure by the alloy only growth of grains is observed, whereas no precipitation processes occur, permits the assumption that for the crystals of this phase the ratio of Te:Sn atoms is the same as for SnTe compound. This suggests that the phase MS3 may be a polymorphic form of SnTe compound. Considering that only reflections of types $\{1\ 1\ 1\}$, $\{2\ 2\ 0\}$ and $\{3\ 1\ 1\}$ occur in the diffractogram, in accordance with the Frevel–Rinn nomogram [11], the ZnS structure accounts for the nature of the diffractogram. This structure has been found, among others, for the metastable phase formed in Cd–Te alloy [12], whose phase equilibrium system is homologous to the Sn–Te system [13]. The shorter distance between the nearest atoms, as compared with the theoretical one, may point to a partly covalent nature of the bond which is characteristic of the ZnS structure. The last transformation most likely represents a polymorphic transition of phase MS3 to SnTe compound. The fact that the transition proceeds at the temperature near to the solidus temperature testifies to the

high stability of phase MS3. Data from the literature indicate [12] that the transition from the ZnS structure to the NaCl structure is difficult, and it has been observed only under conditions of high temperatures or high pressures.

On the grounds of the present results and from the above discussion, the following schema of decomposition of the amorphous phase obtained in Te-20 at.% Sn alloy by rapid cooling from the liquid state is proposed.



MS1 = disordered compound SeTe supersaturated with tellurium atoms; $a = 3.20 \text{ \AA}$
 MS2 = Te (Sn) solution, hexagonal structure; $a = 4.45 \text{ \AA}$, $c = 5.85 \text{ \AA}$
 MS3 = probably ZnS structure type; $a = 6.05 \text{ \AA}$

Acknowledgement

We thank Professor N. J. Grant, Professor B. C. Giessen and Dr H. Jones for helpful comments and discussions. Thanks are also due to Dr M. Lasocka for her help with the DSC analysis. We would like to express our gratitude to Dr I. Jampoler for her help with the translation of this paper. This work was supported by the US National Science Foundation under Grant GF 42 176.

References

1. M. KACZOROWSKI, B. DABROWSKI and H. MATYJA, *Mater. Sci. Eng.* **29** (1977) 189.
2. M. KACZOROWSKI, J. KOZUBOWSKI, B. DABROWSKI and H. MATYJA, *J. Mater. Sci.* (to be published).
3. P. DUWEZ and R. H. WILLENS, *Trans. AIME* **227** (1963) 362.
4. M. L. RUDEE, *Thin Solid Films* **12** (1972) 207.
5. A. HOWIE, O. L. KRIVANEK and M. L. RUDEE, *Phil. Mag.* **27** (1973) 235.
6. S. R. HERD and P. CHAUDHARI, *Phys. Stat. Sol.* **A26** (1974) 627.
7. P. CHAUDHARI, J. F. GRACZYK and S. R. HERD, *Phys. Stat. Sol. B* **51** (1972) 80.
8. A. T. BALCERZAK, C. W. DAWSON, K. K. McCABE and S. L. SASS, Proceedings of the VIIth Congress on Electron Microscopy, Vol. II, edited by P. Favarth, Grenoble (1970) p. 483.
9. B. C. GIESSEN, private communication.
10. "Methodes et Techniques Nouvelles d'Observation en Metallurgie Physique," edited by B. Jouffrey (Société Française de Microscopie Electronique, Paris, 1972) p. 452.
11. S. S. GORELIK, L. N. RASTORGUEV and JU. A. SKAKOV, "Rentgenograficheskij i Elektronograficheskij Analiz Metallov" (Izd. Metallurgizdat, 1963) p. 49.
12. W. B. PEARSON, "A Handbook of Lattice Spacings and Structures of Metals and Alloys," Vol. 2 (Pergamon Press, Oxford, 1967) pp. 93-494.
13. M. HANSEN and K. ANDERKO, "Constitution of Binary Alloys" (McGraw-Hill, New York, 1958) p. 444.

Received 9 August and accepted 16 September 1977.